

CT Arthrography, MR Arthrography, PET, and Scintigraphy in Osteoarthritis

Patrick Omoumi, MD^{a,b}, Gustavo A. Mercier, MD, PhD^c,
Frédéric Lecouvet, MD, PhD^a, Paolo Simoni, MD^a,
Bruno C. Vande Berg, MD, PhD^{a,*}

KEYWORDS

- CT arthrography • MR arthrography • PET • PET-CT
- Scintigraphy • Osteoarthritis • Cartilage

Damage to articular cartilage is considered to be the hallmark of osteoarthritis (OA), even if other factors are involved in the pathogenesis of the disease. The radiological assessment of OA has been based mostly on the radiographic grading of the joint space width, an indicator of cartilage thickness, and on indirect signs such as osteophytes.¹⁻³ Attempts have been made to better delineate cartilage lesions by using intraarticular contrast material in arthrography,⁴ which has inherent limitations due to the projection of three-dimensional structures on a plane. The advent of cross-sectional imaging enabled arthrography to develop further.⁵⁻⁷ Indeed, arthrographic techniques such as computed tomography (CT) arthrography and magnetic resonance (MR) arthrography, thanks to their high resolution and the possibility of multiplanar imaging, remain superior to conventional MR imaging for the delineation of surface lesions of all cartilage areas. However, MR imaging is the only technique enabling the analysis of the internal structure of cartilage, and many recent developments include biochemical qualitative assessment.²

The development of nuclear medicine techniques have focused mainly on the subchondral changes associated with OA, because there are

no radiopharmaceuticals to image the articular cartilage in clinical practice.

We review technical aspects of CT arthrography and MR arthrography of various joints, compare both methods, and report on their most common and useful indications, as well as their pitfalls and limitations. We also describe in detail the nuclear medicine methods that might be relevant for OA research and clinical application.

CT ARTHROGRAPHY AND MR ARTHROGRAPHY *Technical Considerations*

Type of contrast material with CT arthrography

CT arthrography can be performed using either a single (iodine) or double-contrast (iodine and air) technique. In the past, air was used with conventional arthrography to distend the joints, which is not necessary when using CT, because the penetration of the air into cartilage lesions is poor when compared with that of fluid. Nowadays, there is a general consensus in using a single-contrast technique, which is easier to perform^{8,9} and probably less painful.¹⁰

Dilution of the contrast material can be achieved with local anesthetics or saline to avoid beam-hardening artifacts. Nevertheless, the dilution

^a Department of Radiology, Cliniques Universitaires Saint-Luc, Université Catholique de Louvain, Brussels, Belgium

^b Department of Radiology, Centre Hospitalo-Universitaire de Tours, Tours, France

^c Department of Radiology, Nuclear Medicine and Molecular Imaging, Boston University Center, Boston, MA, USA

* Corresponding author.

E-mail address: vandeberg@rdgn.ucl.ac.be (B.C. Vande Berg).

mainly depends on the radiologist preference and investigated joint.^{11–17}

Type of contrast material with MR arthrography

The contrast material of choice for MR arthrography is gadolinium-based (gadolinium-DTPA). It is possible to perform either indirect (less invasive, intravenous gadolinium-DTPA injection) or direct MR arthrography (intraarticular gadolinium injection). For the study of cartilage, the intraarticular injection of contrast material is favored because it allows joint repletion, thus, better delineation of superficial cartilage defects.¹⁸ Other types of contrast material have also been tested, such as saline combined with T2-weighted MR imaging, but gadolinium provides the best contrast-to-noise ratios.^{19–21} A metaanalysis of 112 published studies found gadolinium-DTPA to be a safe and efficient technique for diagnosing internal derangement of joints.²²

Many studies have focused on determining the best gadolinium-DTPA concentration and temporal behavior of intraarticular contrast after injection. At 1.5 T, a concentration of 2–2.5 mmol/L is considered best for imaging to be performed within about an hour after injection.^{22,23} At 3.0 T, a slightly greater dilution may be useful.²⁴ Aspiration of joint effusion before injection can prevent excessive dilution of contrast material, but this is usually not a problem in clinical practice.^{24,25}

It has been shown that iodinated and gadolinium-based contrast material can safely be mixed, and combined MR arthrography and CT arthrography examinations have successfully been obtained for comparison of both studies (Fig. 1).^{26–29} However, at 3.0 T, the presence of iodinated contrast agents has to be minimized, because signal-to-noise peak levels are lower at 3.0 T than at 1.5 T.²⁴

Volume of contrast material

The volume of injected contrast material necessary for proper capsular distention varies according to the joint and is the same for all arthrographic techniques. As a rule, adequate distention is indicated by increased resistance to injection or retrograde flow of contrast material into the needle after disconnection of the syringe.³⁰ The injection should be stopped if the patient has pain.

Injection technique

The injection is usually performed under fluoroscopic guidance,^{16,30} but other injection techniques have been described, using CT,^{16,31} ultrasound,^{32–34} MR³⁵ guidance, or even by using

surface landmarks.^{36–38} The choice relies on the radiologist's preference and on the equipment available. The injection technique follows standard arthrographic procedures, which have been widely described in the literature.^{39–41}

Time delay between the injection of contrast material and imaging

Once injected in the joint, the concentration of contrast materials rapidly decreases by diffusion into the cartilage and synovium, resorption, and fluid influx into the joint.⁴² It is recommended to perform the CT within 30 minutes and the MR within an hour after the contrast injection.^{23,29,43,44} The time delay, however, varies according to the joint. The use of epinephrine in adjunction to the injected material (for instance by mixing 1 mL of a 0.1% solution containing 1 mg of epinephrine with 10 mL of contrast material⁴⁵) slows down the resorption of the latter.^{46,47} However, the use of epinephrine may increase postarthrographic morbidity.¹⁰ Use of epinephrine is usually not necessary with MR arthrography.⁴⁸

It has been shown for the shoulder that exercise has no beneficial or detrimental effect for MR arthrography.⁴⁹ However, in our experience, active and passive full-range articular motion after the injection allows the contrast material to completely cover cartilage surfaces.⁵⁰

Acquisition parameters

CT arthrography exposes the patient to ionizing radiation. Radiation doses should be kept to a minimum, especially in regions close to sensitive areas such as the shoulder (Fig. 2) (thyroid) and the hip (gonads), at the expense of signal-to-noise ratio. The minimal field-of-view should be selected. In knee CT arthrography, for instance, the suprapatellar recess should not be imaged (Fig. 3). Synovial and intraarticular pathologies are depicted on conventional radiographs obtained early after intraarticular injection, before imbibition occurs and masks synovial masses. These radiographs in the case of the knee will cover the suprapatellar recess not imaged by CT.

The CT acquisition parameters include narrow collimation, low-pitch values, and a high milliamperere-second value to obtain high resolution isotropic multiplanar reformats.⁵¹ The reconstructions use bone algorithms, providing high spatial resolution images, and bone windowing is used to view the images. Posttreatment of these high-resolution isotropic images may include curved and maximum-intensity projection reformatting (Fig. 4). Metallic artifacts can be diminished and, more generally, signal-to-noise ratio can be

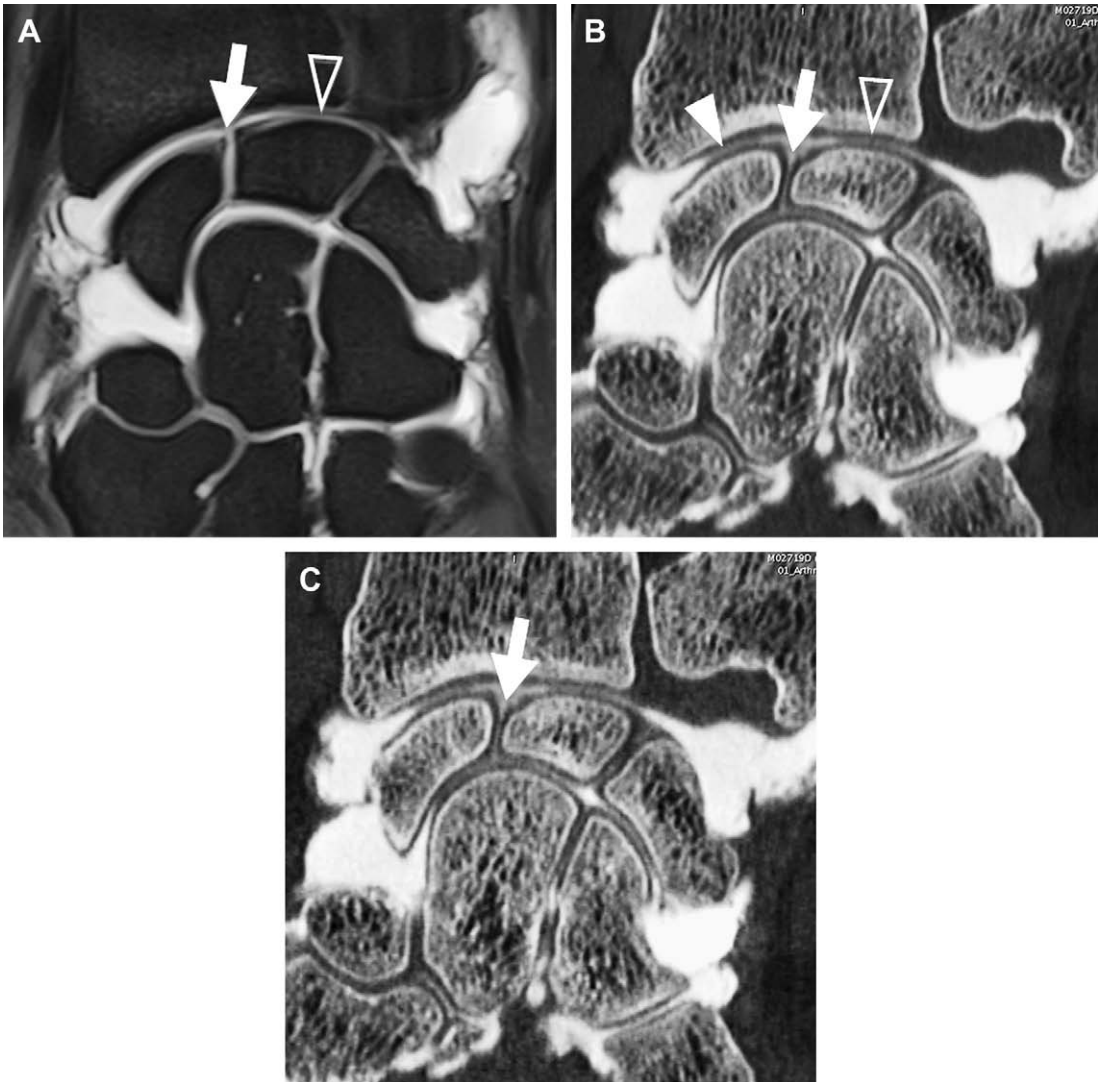


Fig. 1. 34-year-old man with history of trauma. Combined CT arthrography and MR arthrography were obtained after intraarticular injection of gadolinium and iodine. Normal aspect of cartilage (*white arrowheads*) and partial tear of central portion of scapholunate ligament (*arrow*). (A) Coronal fat-suppressed spin-echo T1-weighted MR arthrography image (669/11 ms, TR/TE) shows normal wrist cartilage with intermediate signal intensity (*arrowhead*). Its surface is smooth and regular. (B) 2.4 mm-thick coronal CT arthrography reformatted image shows normal hypodense cartilage, well delimited by the underlying subchondral bone and the intraarticular contrast material at its surface. (C) A 0.6 mm thick coronal CT arthrography reformatted image obtained from same examination demonstrates the same findings. Retrospectively increasing the reformat thickness [from (C) to (B)] leads to an increase of the signal-to-noise ratio. Note that the thickness of the cartilage is easier to evaluate at CT arthrography than at MR arthrography, with better coverage of cartilage surface areas by the contrast material at CT arthrography (*open arrowheads*).

increased by retrospectively increasing the thickness of the reformats and, at the expense of spatial resolution, by using soft tissue algorithms^{52,53} (see **Fig. 1**). Metallic artifacts usually remain mild on new generation CT scanners compared with MR imaging, which makes CT arthrography more suitable for postoperative

patients who have metallic hardware near the joint (**Fig. 5**).^{8,54}

MR arthrography typically includes fat-suppressed spin-echo T1-weighted sequences in three planes, associated to at least one fluid-sensitive sequence for bone marrow edema and extraarticular fluid collections.⁵⁵



Fig. 2. 40-year-old man with shoulder instability. (A) Axial fat-suppressed spin-echo T1-weighted MR arthrography image (786/12 ms, TR/TE) shows cartilage abrasion (grade 4 cartilage loss) of the anterior part of the glenoid (arrow). (B) Axial CT arthrography reformat shows the same chondral lesion (arrow). However, the use of low radiation doses as in this image lead to low signal-to-noise ratio. Note the presence of labral lesions (arrowheads).

Three-dimensional gradient-echo sequences can also be performed and allow multiplanar reformatting.⁵⁶

Risks

As with any other arthrographic procedure, CT arthrography and MR arthrography present risks related to the puncture (infection) and to the injected contrast material (allergic reaction).⁵⁷ However, the risk of infection is quite low (with one infection out of 25,000 arthrograms, according to Berquist,⁵⁸ and three cases of iatrogenic septic arthritis out of 126,000 arthrographic procedures, according to Newberg and colleagues⁵⁷). The risk of severe systemic allergic reactions is also low, although minor reactions can occur.⁵⁸

Moreover, as with other invasive techniques, there is a risk for vasovagal reactions and pain. The best prevention for vasovagal reactions is good communication with the patient and preparation of the injection material out of the patient's sight.⁵⁹ In a recent study evaluating pain and other side-effects of MR arthrography, Saupé and colleagues⁶⁰ concluded that mild postarthrographic pain is most pronounced 4 hours after the procedure, and disappears within 1 week. The origin of postarthrographic pain is debated.⁶¹ It may depend on the nature of the iodinated contrast material for CT arthrography (higher with double contrast CT arthrography,¹⁰ ionic contrast material (probably due to a higher sodium content),^{10,12,62} and the use of epinephrine^{10,63}).

The arthrographic procedure is generally well-tolerated by patients. In a study by Binkert and

colleagues,⁶¹ the arthrographic procedure was better tolerated than the MR imaging examination itself.

In addition to those risks, there is patient radiation exposure with CT arthrography but not with MR arthrography.

Role in Osteoarthritis

Internal structure and cartilage thickness

At CT arthrography, the normal hyaline cartilage appears as a low attenuating structure. The internal contrast of cartilage does not present any variation in its density at CT arthrography, and purely intrachondral lesions, without communication with the surface, cannot be detected (Fig. 6).³ On spin-echo T1-weighted MR imaging, cartilage demonstrates low-to-intermediate signal intensity. Purely intrachondral lesions are barely seen on those sequences. However, fluid-sensitive sequences such as fast spin-echo T2-weighted images acquired during MR arthrography allow detection of concealed lesions of cartilage.

Cartilage loss and thinning are one of the hallmarks of OA. CT arthrography is the most accurate method for the evaluation of cartilage thickness, thanks to its spatial resolution and high contrast between the low attenuating cartilage and its high attenuating deep (subchondral bone) and superficial (contrast material filling the joint) boundaries (see Fig. 1). Indeed, CT arthrography is more accurate than MR imaging even when using cartilage sensitive sequences such as



Fig. 3. 23-year-old man with history of trauma. CT arthrography clearly shows filling of a chondral defect (*arrow-head*) by contrast material in lateral patellar facet on axial (*A*) and sagittal (*B*) reformats. This defect is underestimated by MR imaging on the corresponding (*C*) axial fat-suppressed intermediate-weighted fast spin-echo image (2200/45 ms, TR/TE) and (*D*) sagittal proton density-weighted spin-echo image (2200/18 ms, TR/TE).

SPGR as shown by cadaveric studies on the ankle.⁶⁴ CT arthrography is also more accurate than MR arthrography for the assessment of cartilage thickness in cadaver hip joints (**Figs. 7 and 8**).¹⁷ CT arthrography has been used as a reference in studies evaluating the accuracy of noninvasive MR imaging sequences for the assessment of cartilage thickness.⁶⁵ However, CT arthrography measurements can be influenced by some technical factors as recently shown by Anderson and colleagues⁶⁶ in a phantom study. The authors suggest the use of lower contrast agent concentrations and the maximization of joint space by completely filling the joint capsule with diluted contrast and/or by applying traction to

the joint. A more recent study concluded that multidetector CT arthrography and MR arthrography are equally accurate in measuring hip cartilage thickness as far as the coronal plane is concerned.⁶⁷

The thickness of cartilage is highly variable from one individual to another, from one joint to another, and from one area of the joint to another. This is particularly true for the knee, where the cartilage is usually thicker in areas with concave subchondral bone and thinner in areas adjacent to the menisci.⁵⁰ In the hips, a cartilage thickness gradient exists from the periphery to the center of the femoral head and from the medial to the lateral edge of the acetabulum (see **Figs. 7**

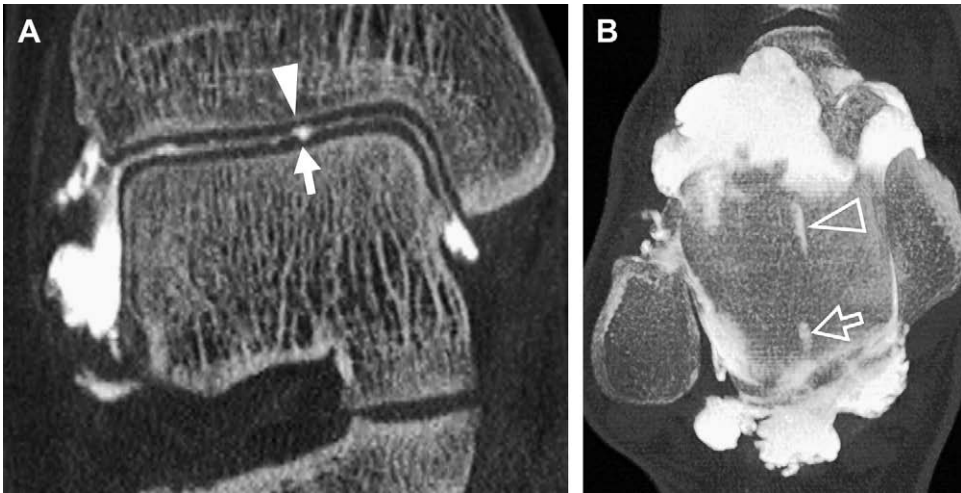


Fig. 4. CT arthrography in a 43-year-old man with history of trauma. (A) Coronal reformat shows a grade 3 (more than 50% in depth) cartilage defect in talar dome (*arrow*) and a grade 2 (less than 50% in depth) defect in the tibial plafond (*arrowhead*). (B) Curved axial maximum-intensity projection image shows the spatial orientation of the cartilage fissure, whose long axis is parallel to the axis of the talar dome (*arrowhead*). Another cartilage defect is seen more posteriorly (*arrow*).

and 8).¹⁷ The inversion of that thickness gradient is an early sign of degenerative OA. In shoulders, glenoid cartilage is physiologically thinner at the center.

Cartilage surface

The normal cartilage surface appears smooth and continuous (see Fig. 1). Some focal physiologic defects, such as the glenoid central defect, the trochlear notch at the elbow, and the stellate lesion

in the acetabulum (see Fig. 8), may exist and should not be mistaken with cartilage lesions. In addition to those focal physiologic defects, some epiphyseal areas are physiologically not covered by cartilage (bare areas).

Focal surface lesions of the cartilage are well depicted with both techniques and appear as areas filled with the intraarticular contrast material (see Figs. 2–4, 9). However, the contrast between the cartilage and the intraarticular contrast material,

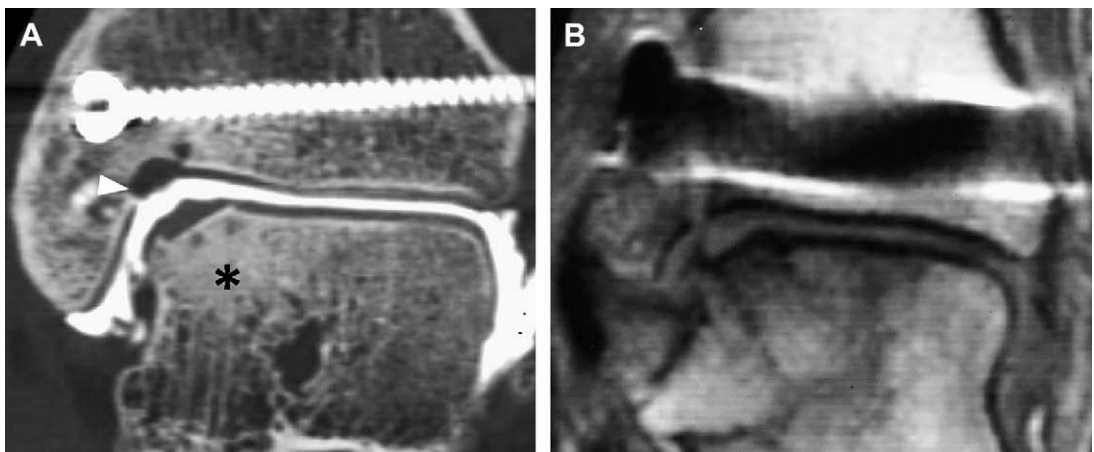


Fig. 5. 40-year-old man with history of traumatic osteochondral lesion of the talus dome, treated with osteochondral grafting. (A) Coronal CT arthrography reformat shows the well-incorporated osteochondral graft (*). Cartilage surface shows minor irregularities and its thickness is acceptable. The graft is well incorporated with no contrast at the interface between the graft and the adjacent talar cartilage. A focal chondral lesion is visualized on the opposite tibial surface (*arrowhead*). (B) Coronal proton density-weighted MR imaging (920/12 ms, TR/TE) shows the cartilage surface is poorly defined in comparison to the CT arthrography image. Note that metal-related artifact is milder on CT arthrography (A) than on MR imaging (B).

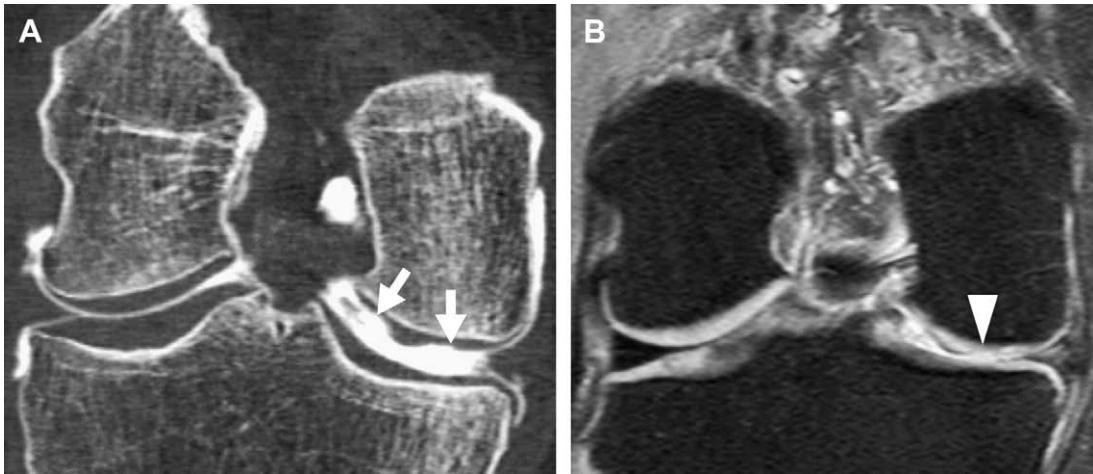


Fig. 6. 46-year-old woman with osteoarthritis. (A) Coronal CT arthrography reformat shows extensive grade 3 chondral loss at the medial femoral condyle (arrows), associated with thinning of the medial tibial plateau cartilage, well delineated by the intraarticular contrast material. (B) Coronal fat-suppressed fast spin-echo intermediate-weighted MR imaging shows irregularity of the chondral surface and chondral signal intensity changes in the medial compartment. The normal variations in cartilage signal intensity of the lateral tibial plateau seen with MR imaging (B) are not detected on the CT arthrography (A). Injection of intraarticular contrast allows distention of the joint space (A) and good delineation of cartilage surface compared with the nonenhanced MR imaging. This allows better characterization of femoral and tibial chondral lesions.

as well as the image resolution, are higher with CT arthrography compared with MR arthrography, leading to a higher degree of confidence in depicting those lesions, and a higher interobserver reproducibility.⁶⁸

Cartilage loss can be either focal or extensive and different terms are used to characterize either the shape or the depth of the defects. Fissures have a linear shape with one diameter being much smaller than the other (see Fig. 4). Cartilage ulcers have a more round shape on an en face view (see Fig. 9). This classification system, based on the shape of the surface defect, has barely been validated. Numerous grading systems of cartilage lesions are derived from the grading systems used at arthroscopy and are mainly based on the following parameters: integrity of cartilage surface and depth of cartilage defects (Table 1).^{15,69–71}

Sensitivities and specificities at chondral lesions depiction are good for thin or thick cartilage.^{9,72} However, CT arthrography is more accurate for thinner cartilage lesions compared with MR arthrography (see Fig. 1).¹¹

CT arthrography and MR arthrography have significantly better sensitivity and specificity for high grade lesions (3 and above) for various joints, such as patellar,³ knee,⁷² elbow,⁶⁸ and shoulder,¹¹ than for more superficial lesions (see Figs. 2, 6–9).

The coverage of the cartilage surface and delineation of opposite cartilage surfaces is poor with

certain joints such as the ankle and hip, and is usually better at CT arthrography than at MR arthrography (see Fig. 1)^{68,73}, leading some authors to propose traction maneuvers.^{64,74}

Subchondral changes

Both CT arthrography and MR arthrography can show subchondral bone changes. CT arthrography is better at depicting subchondral bone sclerosis and osteophytes (see Figs. 7 and 8). Both techniques can show central (nonmarginal) osteophytes, associated with more severe changes of OA than marginal osteophytes.^{75,76} MR arthrography is the only technique allowing depiction of subchondral bone marrow edema-like lesions on the fluid-sensitive sequences usually acquired along the T1-weighted sequences. This depiction is usually a sign of high-grade cartilage lesions (see Fig. 9).⁷²

PET AND SCINTIGRAPHY

Tracers and Imaging Technologies

Even though it may not be the first step in the pathology of OA, damage to the articular cartilage remains the hallmark of the disease.⁷⁷ In clinical practice there are no radiopharmaceuticals to image articular cartilage, but selenium-based tracers are under development for this purpose.^{78–80} Radiopharmaceuticals that are available for clinical imaging target secondary

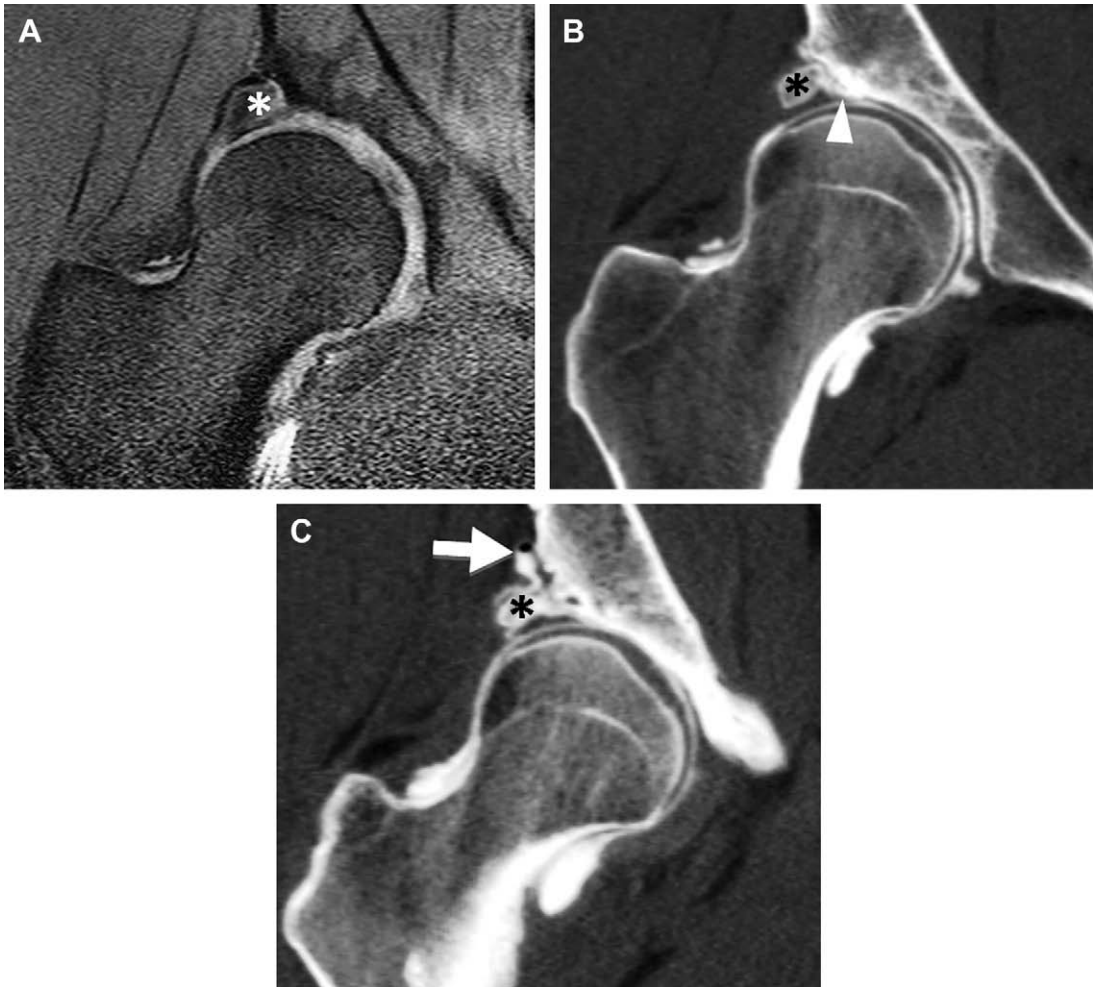


Fig. 7. 39-year-old woman with dysplastic hip. (A) Coronal fat-suppressed spin-echo T1-weighted MR arthrography image (489/12 ms, TR/TE) shows acetabular chondropathy and bony fragment (*) separated from the acetabular margin by contrast material. (B,C) Coronal CT arthrography reformats clearly show a down-to-bone cartilage defect (*arrowhead*) on the lateral margin of acetabulum and acetabular bony fragment (*). On CT arthrography image, the bone fragment is easily recognized but the contrast material at the bone–acetabular interface is less well depicted than at MR arthrography. The contrast material between the acetabulum and the femoral head is better seen at CT arthrography than at MR arthrography. Accumulation of contrast material at the margins of the acetabulum (*arrow*) is well seen in (C). Femoral head cartilage is normal, with a preserved gradient of cartilage thickness from the periphery to the center of the femoral head.

features of OA that are associated with damage to the articular cartilage, primarily bone turnover changes seen with osteophyte formation, subchondral sclerosis, and subchondral cyst formation.^{81,82} Inflammation is a minor element of OA with the exception of the erosive OA seen in the hands, and this has also been the target of imaging with radiopharmaceuticals.⁸¹

Strategies that focus on bone imaging are more widespread, and diphosphonate derivatives radiolabeled with Tc-99m are the primary agents for this imaging. They have the added value that a modicum of soft tissue imaging is still possible

with these agents when a radionuclide angiogram and blood pool acquisition is added to the routine delayed views (ie, imaging done in three phases).

Two diphosphonates are in common use: Tc-99m methylene diphosphonate (Tc-99m MDP; Tc-99m medronate) and Tc-99m hydroxymethylene diphosphonate (Tc-99m HDP; Tc-99m oxidronate). These radiopharmaceuticals have a proven track record since their introduction in the 1970s, and are readily prepared from kits available from suppliers around the world. The agents have significant affinity to bone, with nearly 50% of the tracer binding to the bone trabeculae through the

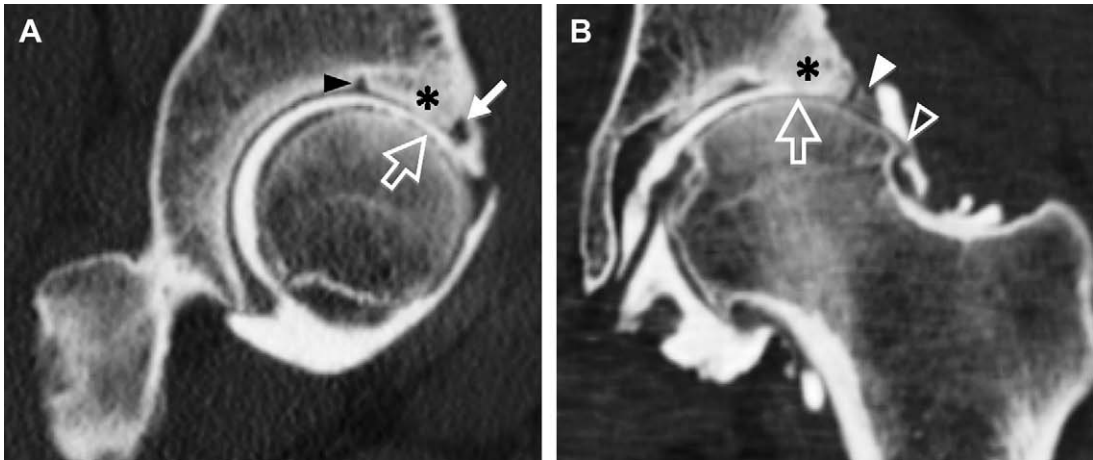


Fig. 8. 45-year-old woman with left hip osteoarthritis. (A) Sagittal and (B) coronal CT arthrography reformats clearly depict typical changes of osteoarthritis in the superolateral and anterior aspects of the hip joint: femoral head and acetabular cartilage thinning (*open arrows*), marginal femoral osteophytes (*open arrowhead*), acetabular osteophytes (*white arrowhead*), subchondral bone sclerosis (***), and subchondral cystic changes (*arrow*). Note the presence of a physiologic stellate defect of the subchondral bone plate at the apex of the acetabular bone (*black arrowhead*, A).

process of chemisorption. They have an excellent safety profile and the standard adult dose of 20–25 mCi results in excellent imaging with acceptable radiation exposure to the patient (approximately

5 mSv/25mCi dose).⁸³ They are readily excreted in the urine. The bladder is the critical organ so frequent voiding minimizes the exposure to radiation. Delayed imaging starts 2–3 hours after

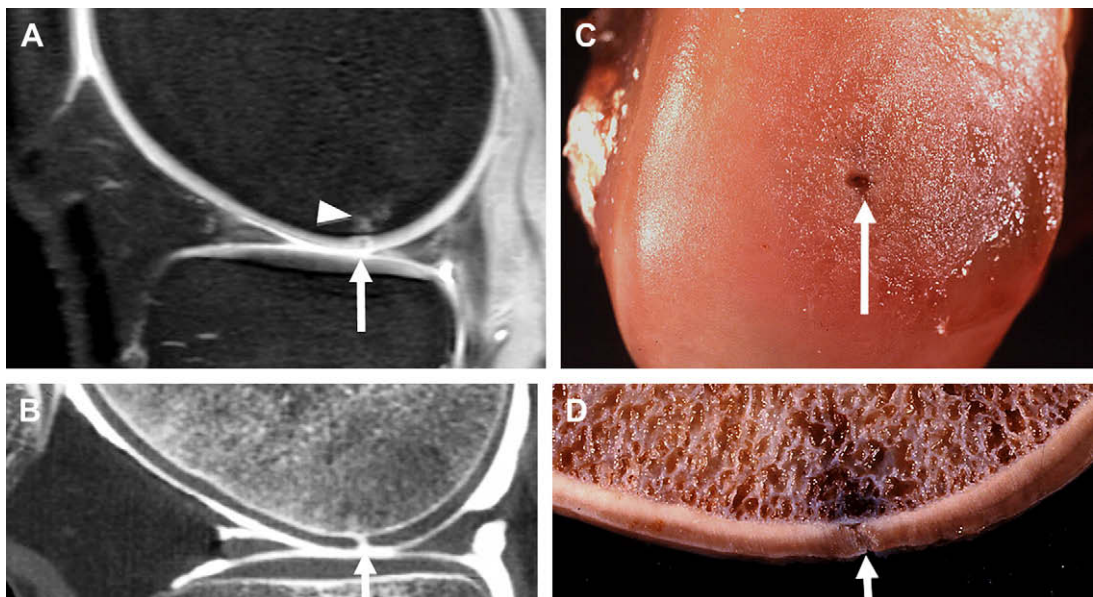


Fig. 9. Cadaveric knee specimen presenting a grade 4 (down-to-bone) chondral ulcer. (A) Sagittal fat-suppressed fast spin-echo intermediate-weighted MR imaging (3400/29 ms, TR/TE) shows grade 4 down-to-bone chondral ulcer (*arrow*) associated with subchondral bone edema (*arrowhead*) in the lateral femoral condyle. (B) Sagittal CT arthrography reformat shows the grade 4 chondral defect (*arrow*) filled with contrast material. Subchondral edema cannot be seen with CT. (C) En face photograph of the specimen shows the focal, round-shaped chondral defect (*arrow*). (D) Close-up photograph of the corresponding anatomic sagittal section shows the down-to-bone defect (*arrow*) in the lateral femoral condyle. Both MR imaging and CT arthrography are accurate for the evaluation of high-grade chondral lesions (grade 3 and above) but CT arthrography cannot demonstrate bone marrow changes.

Table 1
Grading systems for cartilage lesions at arthroscopy and CT and MR arthrography

Grade	Arthroscopic Findings	CT and MR Arthrography
Grade 0	Normal	Smooth surface and normal thickness of cartilage
Grade 1	Fibrillation without cartilage loss and cartilage softening	Smooth surface and normal thickness of cartilage
Grade 2	Substance loss less than 50% of cartilage thickness	Penetration of contrast in cartilage to less than 50% in depth
Grade 3	Substance loss more than 50% of cartilage thickness but not down-to-bone	Penetration of contrast in cartilage to more than 50% in depth
Grade 4	Down-to-bone cartilage loss	Penetration of contrast down to subchondral bone

injection to allow for clearance from the soft tissues. Imaging is earlier with Tc-99m HDP, given its higher affinity for bone. However, Tc-99m HDP is more expensive than Tc-99m MDP.

Another bone imaging agent is 18-Fluoride (18-F⁻), a positron-emitting radioisotope that predates the diphosphonates compounds.⁸⁴ However, it is only now, with the widespread acceptance of positron emission tomography (PET) and PET-CT technologies, that it is possible to exploit this agent in clinical imaging.⁸⁴ This radioisotope is readily produced in a cyclotron, and has high affinity to bone through the process of anion substitution in the hydroxyapatite complex. Bone images of high quality are readily obtained using modern PET-CT scanners as early as 30 minutes after injection of 5–10 mCi of tracer. Excretion is through the urine, and nearly 50% of the tracer binds bone.^{83,84} The estimated whole body dose is 10 mSv/10 mCi dose. As of January 1, 2008, changes to the clinical procedural terminology of the American Medical Association in the United States allows physicians to bill insurance companies for 18-F⁻ PET (and PET-CT) imaging.⁸⁵

Radiopharmaceuticals that image soft tissue components and largely target the inflammatory component of OA include radiolabeled white blood cells, Gallium-67 citrate, and 18-fluorodeoxyglucose (18-FDG). White blood cells labeled with Tc-99m or In-111 and Gallium-67 citrate are gamma photon emitters that are used in detecting infection and inflammation. They may have a role in imaging of septic arthritis, and possibly inflammatory arthritides, but are not used in imaging OA, and therefore not discussed in this review.^{86–88} 18-FDG is a positron-emitting radiopharmaceutical that accumulates at sites of increased glucose metabolism, particularly due to increase in glucose transporters, and to increase in aerobic glycolysis as seen in tumor cells and activated leukocytes.^{89,90} Although

18-FDG is used primarily for imaging in oncology, it has also been applied to infection and inflammation imaging, including bone infections.^{87,91} The PET in the 18-FDG PET-CT scans of subjects referred for cancer imaging shows uptake at sites of OA in the CT part of the examination. Recent reports suggest a possible role for 18-FDG to detect and possibly evaluate the inflammatory component of OA.^{92–94}

To image the joints there are a variety of methods in nuclear medicine. In addition to three-phase bone scans, delayed views with planar scintigraphy or single-photon computed tomography (SPECT) are common (Fig. 10).⁹⁵ Magnification imaging with pinhole collimators (see Fig. 10) provides details in planar scintigraphy.⁹⁶ Today, PET imaging is done largely in whole body PET-CT scanners capable of hardware fusion of anatomic and physiologic images, as well as the attenuation correction necessary for quantitative imaging.⁹⁷ Similar hybrid imaging has been developed for SPECT, and, as expected, is labeled SPECT-CT.^{98–101} There are new small part PET scanners designed for breast imaging¹⁰² that are being evaluated for joint imaging using either 18-F⁻ and/or 18-FDG. An example is the PEM Flex Solo II PET scanner (Naviscan PET Systems, Inc., San Diego, California) (Fig. 11).¹⁰³ These scanners have exquisite sensitivity and higher resolution than whole body scanners. They promise to extend PET imaging into new areas, including joint imaging, but at this time remain the subject of research.

Applications

Diphosphonate imaging

Although the role of scintigraphy in the diagnosis of OA is not clear, rheumatologists find bone scans useful in their practice,¹⁰⁴ because bone scintigraphy is a simple examination that allows for

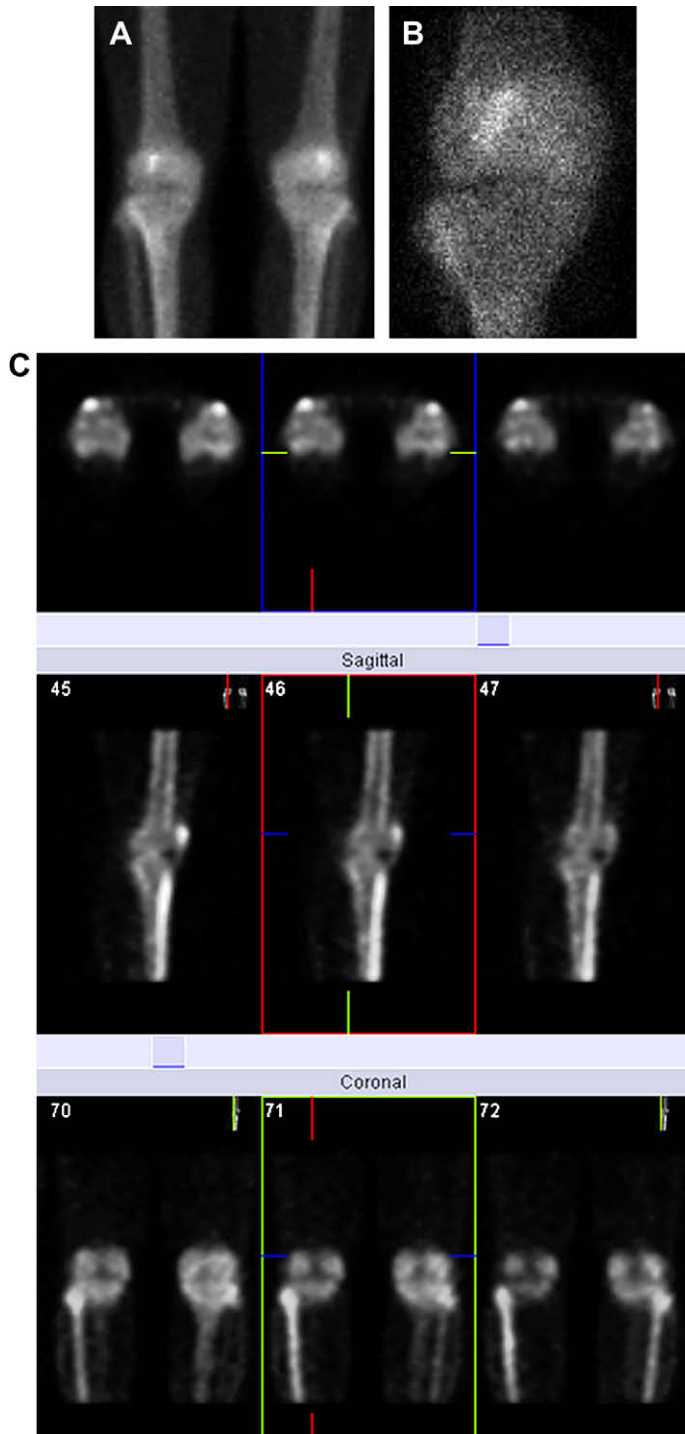


Fig. 10. Asymptomatic 48-year-old male volunteer. (A) Anterior projection of 5-hour delayed 25 mCi Tc-99m MDP scintigram. (B) Magnification pinhole image of the right knee in (A). (C) Selected nonattenuation corrected SPECT views in axial (*upper row*), sagittal (*middle row*), and coronal (*lower row*) planes through the right knee. There is no activity in the joint but uptake is seen in the anterior surface of both patellae, and the SPECT scans shows narrowing of the tibiofemoral joint on the left side with no increased uptake.



Fig. 11. PEM Flex Solo II Clinical System configuration. (Courtesy of Naviscan PET Systems, Inc., San Diego, CA; with permission.)

a full body survey that helps to discriminate between soft tissues versus bone/joint origin of pain, and to locate the site of pain in patients with complex symptoms. An analysis by Duncan and colleagues¹⁰⁴ of the practice of Australian rheumatologists found that bone scans altered clinical diagnosis and changed the course of management over 30% of the time. More important, it prevented further investigations in 60% of the cases.

In the specific case of “unclassified arthritis,” Duer and colleagues¹⁰⁵ have shown that a combination of MR imaging of the hands and wrists and Tc-99m HDP whole body scintigraphy is useful to discriminate between the different arthritides. They evaluated a cohort of 41 subjects that remained unclassified after applying conventional clinical, biochemical, and radiographic methods, including the American College of Rheumatology criteria for rheumatoid arthritis (RA). Discrimination between the different RA and OA was done on the basis of the distribution of joint uptake seen in the bone scans, and the presence of synovitis and erosions in the MR imaging scans. The gold standard was specialist review 2 years after initial imaging and evaluation. The combination of MR imaging and scintigraphy was 95% accurate in discriminating between RA and non-RA. Although their intent was to help with the early diagnosis of

RA, none of the eight subjects originally classified as OA on the basis of their imaging algorithm were reclassified by the gold standard.

It is clear that scintigraphy has high sensitivity in detecting bone reaction to the pathology of OA.^{82,106–108} It is important to recognize that bone scintigraphy with diphosphonates targets the bone response that results from the abnormal biomechanics of joint motion when the articular cartilage is damaged. The physiology of this uptake has been reviewed by Merrick,⁸² who observes that uptake is related to osteophyte formation, subchondral sclerosis, and subchondral cyst formation that all result from abnormal loads on the joint. When osteophyte formation is successful in reducing the point forces that result from cartilage damage, tracer uptake may stop as the osteophyte matures and no new osteophytes are formed. It is noteworthy that uptake associated with subchondral sclerosis correlates well with increases in bone marrow signal in T2-weighted MR imaging, and that the agreement between bone uptake and MR imaging features of osteophytes or cartilage defects is less striking.^{82,109}

Therefore, it is not surprising that bone scans show abnormal uptake before the detection of abnormal morphology in routine radiography (Fig. 12).^{82,106,107} Also, activity in bone scintigraphy implies that abnormal stress persists and that the disease will progress.⁸² For this reason, some advocate the use of scintigraphy to select candidates for clinical trials that evaluate disease-modifying drugs. In clinical practice, a negative bone scan may provide some reassurance that disease is unlikely to progress in the next 5 years, although the predictive power of scintigraphy is far from 100%.¹¹⁰ Indeed, recent work by Mazzuca and colleagues^{108,111} demonstrates that similar or better predictive power for progression of disease can be obtained by combining indices of clinical symptoms with radiographic methods that are common in the research setting, namely measurement of joint space narrowing using standard projections and computer-assisted measurements. His approach provides a simpler and safer alternative to scintigraphy in selecting patients that are likely to progress in their disease, because it avoids the whole body radiation dose that results from injecting a radiotracer. However, his radiographic methods are uncommon in routine clinical imaging departments.

In addition to assisting in the diagnosis and prognosis of OA, scintigraphy may also assist in therapy. Facet OA of the spine can lead to back pain that responds to the injection of

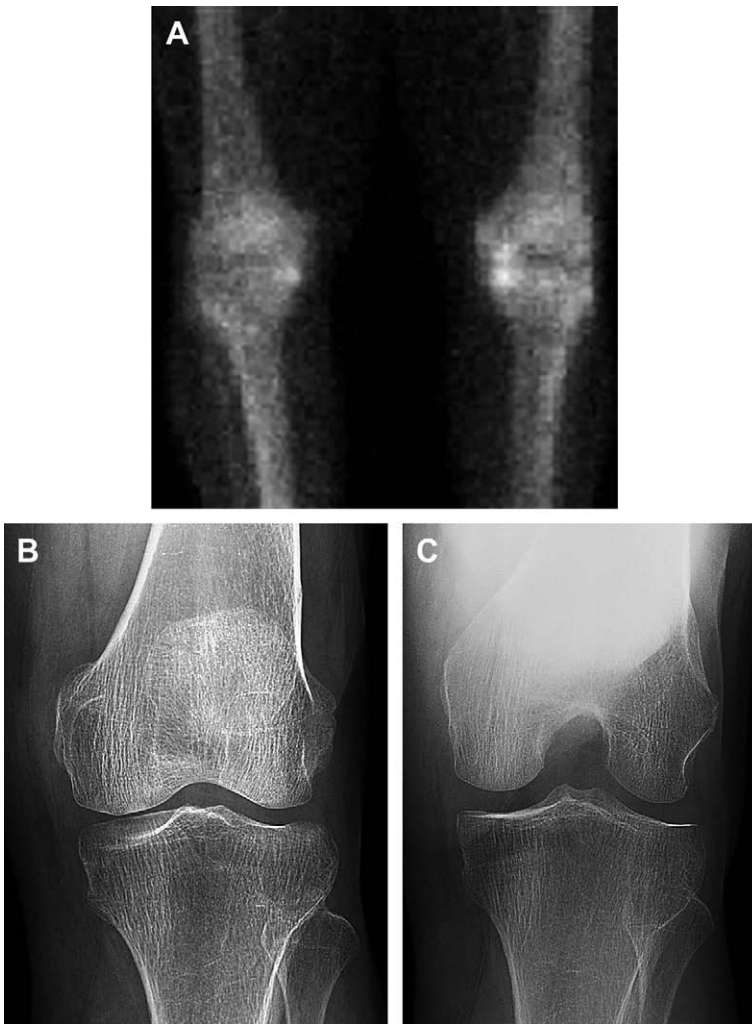


Fig. 12. Left knee pain in middle-aged woman. (A) 3-hour delayed 25 mCi Tc-99 MDP bone scan in the anterior projection shows uptake in the medial compartments is worse on the left side. This is compatible with osteoarthritis. However, (B) posteroanterior and (C) tunnel view radiographs show no significant findings.

steroids.^{112,113} Early work by Dolan and colleagues¹¹³ demonstrated that spine SPECT imaging with diphosphonates is able to select those facets that will respond to steroid injections (Fig. 13). In the authors' experience, this technology is most useful when studies are read in conjunction with CT myelograms or MR imaging that allow for evaluation of disc disease. Good physical examination is imperative to confirm that imaging findings are compatible with the patient's pain. Recently Kim and Park described a pattern of uptake in planar scintigraphy of the lumbar spine that is so characteristic of facet OA that it renders SPECT unnecessary.¹¹⁴ In this pattern, bilateral facet uptake at the same axial level leads to a characteristic "V" shape to the uptake in the posterior view. However, it is likely that this pattern has low sensitivity and SPECT imaging is necessary when the pattern is not seen in a patient with back pain.

As of now, imaging with diphosphonates is dominated by planar scintigraphy. SPECT imaging has better sensitivity and improves anatomic localization. A recent study confirmed the ability of SPECT to detect early osteoarthritis of the knee with good correlation to clinical findings.¹¹⁵ Due to its improved anatomic localization, SPECT of the knee has also proven useful in planning unicompartmental knee arthroplasty of the medial compartment of the tibiofemoral joint, because it is in this compartment that scintigraphic findings correlate best with those features of OA detected at the time of surgery.¹¹⁶ SPECT-CT imaging allows for attenuation correction that may lead to quantification and improves specificity.^{98,100,101} Recent literature illustrates how the hybrid technology improves bone imaging, because the CT not only improves the quality of the scintigraphic imaging, but also leads to the characterization of commonly nonspecific scintigraphic

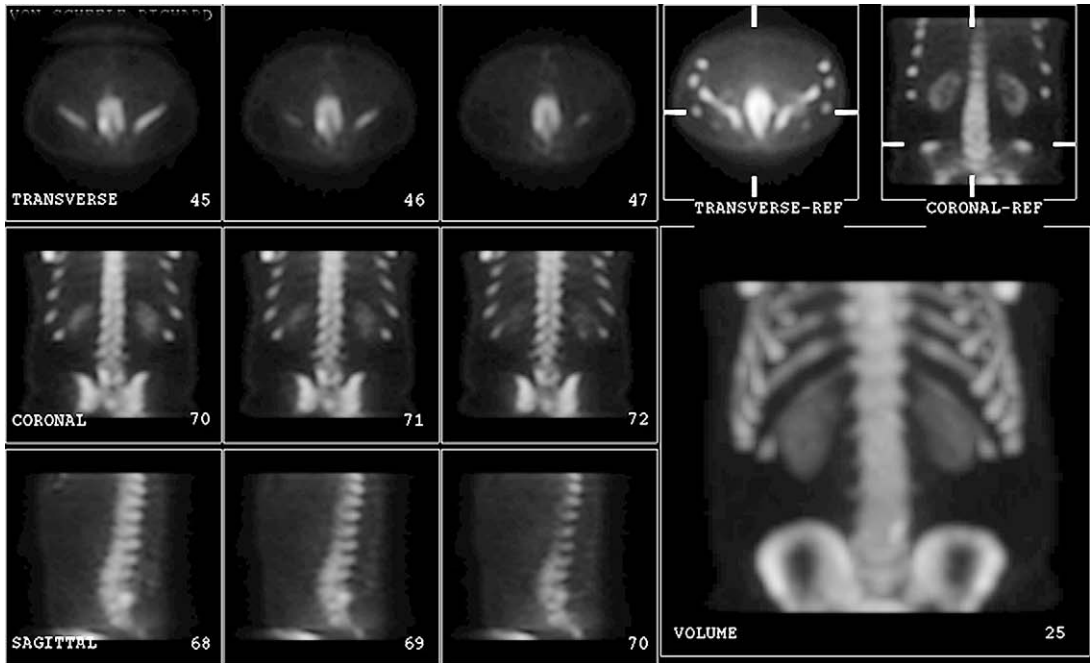


Fig. 13. Selected views from a nonattenuation corrected 3-hour delayed 25 mCi lumbar spine SPECT scan show uptake in the right facet joint at the L4-L5 level. The maximum intensity projection imaging on the right lower corner is seen from the posterior view.

uptake.^{98,99,101,117} Resolution recovery methods allow for faster SPECT imaging or improved quality when the imaging time is unchanged.^{118,119} This feature is already being offered by several

manufacturers. Pinhole collimation is time-consuming, but it affords details seen more often in pediatric applications,⁹⁶ though seldom applied to adults with arthritis (see **Fig. 10**). For the most

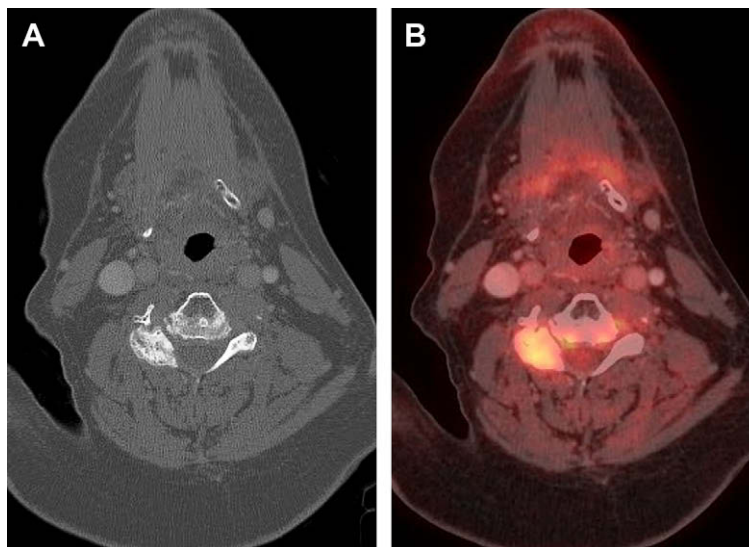


Fig. 14. 62-year-old man treated for hypopharyngeal cancer who presents to 18-FDG PET-CT for restaging. (A) Axial CT scan shows clear evidence of advanced OA in a right facet of the cervical spine. (B) Axial fused 18-FDG PET-CT scan (10 mCi 18-FDG with 60 minutes' incubation before imaging) shows the intense 18-FDG uptake of the osteoarthritic cervical facet.

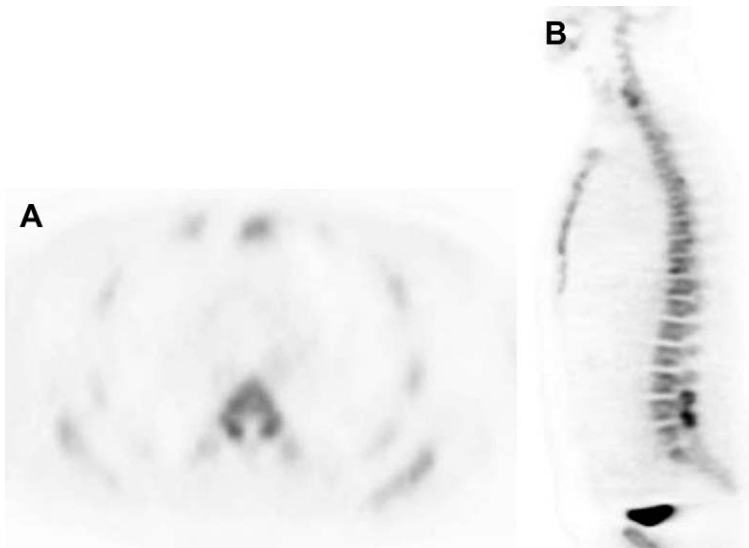


Fig. 15. Selected axial and sagittal views from a 90-minute delayed 10 mCi 18-Fluoride PET scan done in a whole body scanner with CT attenuation correction show facet uptake consistent with L3-L4 and L4-L5 osteoarthritis. Contrast the quality of these images with the SPECT scan in [Fig. 13](#).

part, none of these methods have found their way into arthritis imaging.

Positron emitters

Musculoskeletal imaging with positron emitters and PET-CT technology is still in its infancy. The effort is largely confined to oncology imaging, but there is no reason to expect that these technologies will not play a role in imaging patients with arthritis. Anecdotal experience with 18-FDG in imaging patients with cancer and two early reports demonstrate that PET with this agent is able to detect OA ([Fig. 14](#)).^{92,93} The uptake is seen in the synovitis associated with OA, and therefore is different from the imaging done with bone-seeking agents. Indeed, it is not surprising that 18-FDG is seen more often in joints affected by RA than OA.⁹⁴

^{18-F} PET and PET-CT imaging improves on the poor resolution of SPECT imaging with diphosphonates while retaining excellent sensitivity. Comparison of [Figs. 13](#) and [15](#) makes it clear that images from the positron emitter are superior to those from the gamma emitter.

Hybrid technologies like PET-CT bring a new element to arthritis imaging and research, because they combine anatomic and functional imaging in ways that no other imaging technologies are able to do. The field would benefit from the development of cartilage-specific agents. Such a radiopharmaceutical combined with 18-FDG and 18-F would bring a new dimension to arthritis imaging, because the applications of these three

tracers would target three major elements in the pathology of OA and arthritis in general: cartilage, inflammation, and bone.

PET scanners to image small parts have been developed specifically to image the breast (see [Fig. 11](#)).¹⁰³ The scanner is noteworthy for its sensitivity and resolution, but lacks attenuation correction, so quantification is not possible as it is with whole body PET-CT scanners. Nevertheless, [Figs. 16](#) and [17](#) show very preliminary images of a normal volunteer imaged using significantly lower doses than those used with whole body scanners. These images are far from optimal, but, using existing technology, they can be improved by tweaking the dose of radiotracer and time to image as illustrated by comparing [Figs. 16](#) and [18](#). The unit is portable, and the cost and operational requirements are significantly less than those for whole body scanners. Time will tell if these units find their way into imaging of joints in a fashion similar to small-parts fixed-field specialty MR imaging units.

SUMMARY

MR imaging currently remains the method of choice for noninvasive diagnosis of chondral lesions. It is the only technique that allows the evaluation of surface lesions, subchondral changes, and the structure of cartilage. Whenever accurate evaluation of surface changes is needed, however, invasive arthrographic techniques are indicated. Compared with MR arthrography, CT

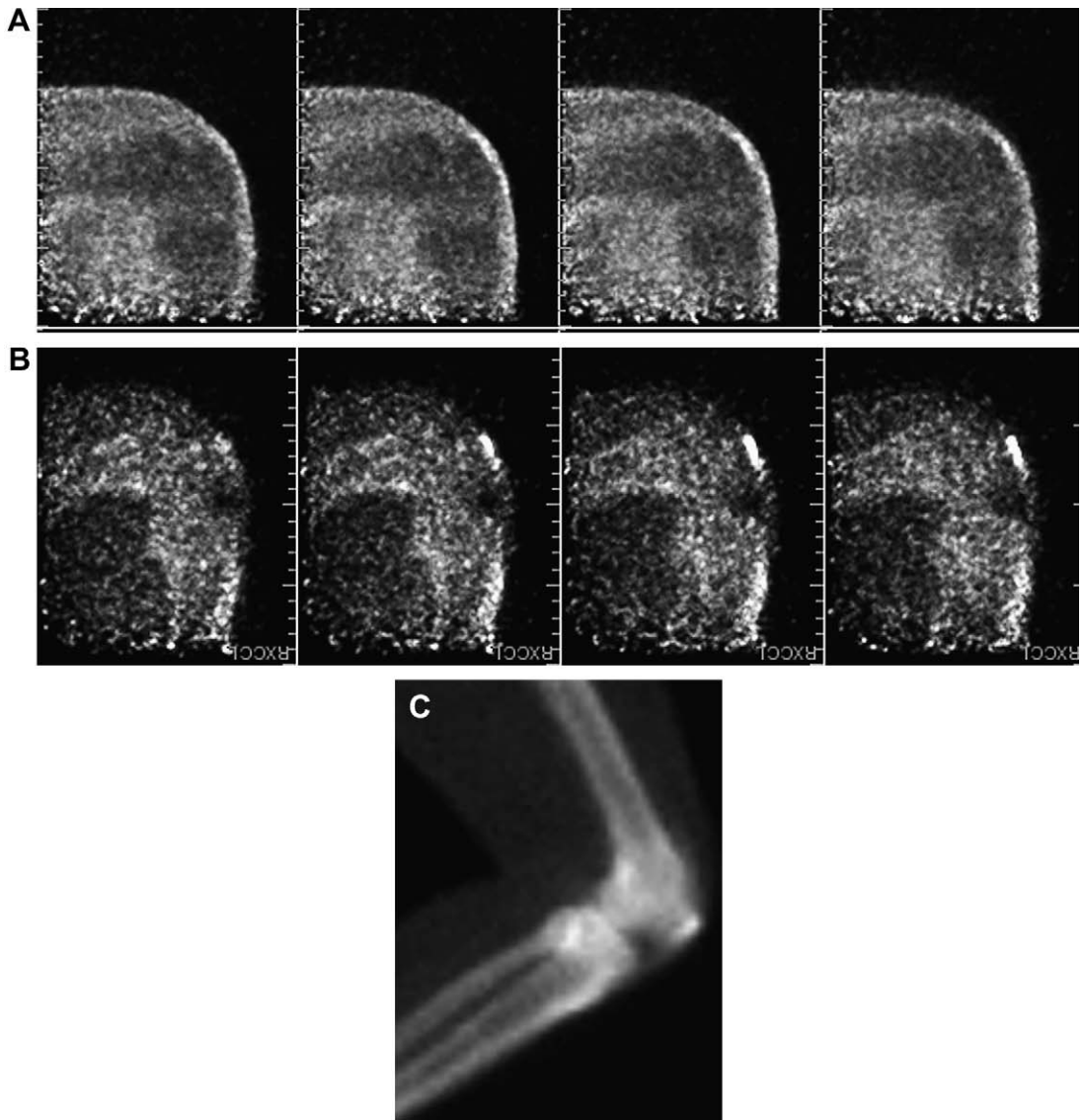


Fig. 16. Right knee of the same asymptomatic volunteer as in Fig. 10. (A) Selected sagittal views of 18-FDG PET scan (4 mCi with 60 minutes' incubation) done with small part scanner shown in Fig. 11 shows no activity in the joint and only apparent tracer uptake in the skin over the patella. (B) Selected sagittal views of 18-Fluoride scan (0.87 mCi with 90 minutes' incubation) using small parts PET scanner and (C) right lateral view of 25 mCi Tc-99m MDP 5-hour delayed scintigram demonstrate no activity in the joint, but uptake is seen in the anterior surface of the patella.

arthrography has the inconvenience of radiation exposure and the limitation to surface lesions only. CT arthrography is, however, a valuable technique whenever MR arthrography is not possible (eg, not available, contraindicated, or technically impossible, such as with obese or claustrophobic patients, or the presence of metallic hardware). The indications of the intraarticular injection of contrast material may evolve in the near future, with the development of new 3.0 T imaging techniques and three-dimensional acquisitions.

Radioisotope methods to image osteoarthritis suffer from the lack of agents that specifically target articular cartilage and the need to use ionizing radiation. However, bone scintigraphy is sensitive to the reaction of the underlying bone when the cartilage is damaged, and a negative bone scan may provide assurance that the disease is unlikely to progress. The advent of 18-FDG PET and PET-CT imaging brings the opportunity to explore the inflammatory component of osteoarthritis. 18-F⁻ PET and PET-CT and Tc-99m MDP/

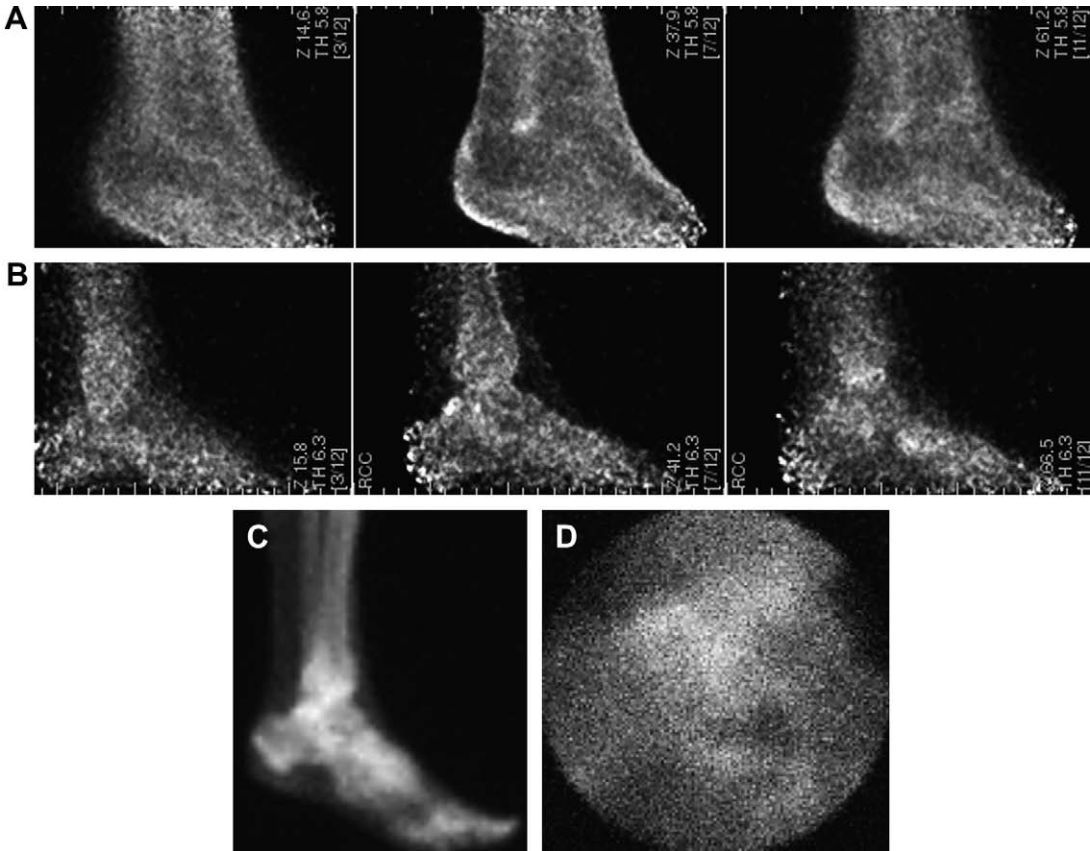


Fig. 17. Right ankle of the same asymptomatic volunteer as in Fig. 10. (A) Selected sagittal views of 18-FDG PET scan (4 mCi with 60 minutes' incubation) done with small part scanner shown in Fig. 11. (B) Selected sagittal views of 18-Fluoride scan (0.87 mCi with 90 minutes' incubation) using small parts PET scanner. (C) Right lateral view of 25 mCi Tc-99m MDP 5-hour delayed scintigram. (D) Magnification pinhole image of the right ankle focusing in the tibiotalar joint. An uptake is seen in the posterior aspect of the talotibial joint in both 18-FDG and bone imaging.

HDP imaging with SPECT and SPECT-CT bring added sensitivity and improved anatomic localization that has not been readily exploited in imaging osteoarthritis. They also bring the opportunity to

combine molecular and anatomic imaging in one image. Small-part PET devices are already in clinical use in breast imaging, and in development for joint imaging. Their value stems from lower

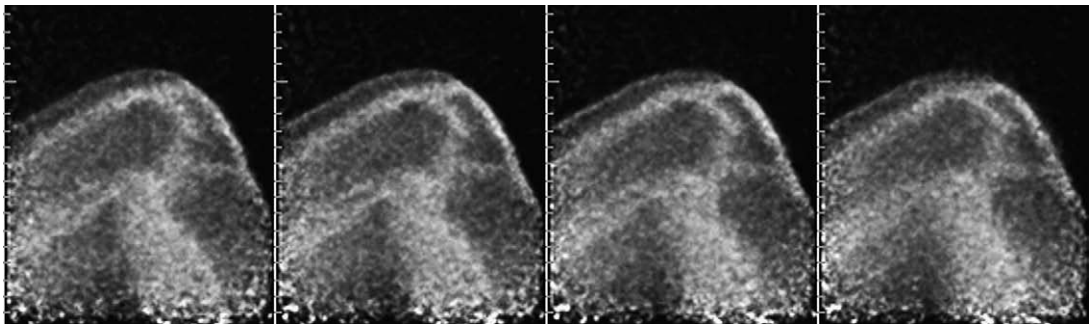


Fig. 18. 79-year-old woman with asymptomatic knee who underwent a restaging of ovarian cancer with 18-FDG PET-CT imaging. Selected sagittal views through one knee using small parts PET scanner (after whole body scan, 100 minutes after injection of 10.6 mCi of 18-FDG) show improved imaging with larger dose and longer incubation period.

operating costs, and lower radiation burden to the patient while still retaining significant resolution and sensitivity.

REFERENCES

1. Drapé JL, Pessis E, Sarazin L, et al. MRI and articular cartilage. *J Radiol* 1998;79(5):391–402.
2. Link TM, Stahl R, Woertler K. Cartilage imaging: motivation, techniques, current and future significance. *Eur Radiol* 2007;17(5):1135–46.
3. Rand T, Brossmann J, Pedowitz R, et al. Analysis of patellar cartilage. Comparison of conventional MR imaging and MR and CT arthrography in cadavers. *Acta Radiol* 2000;41(5):492–7.
4. Daniel E, Lajko P. Diagnostic significance of the positive arthrography in injuries of the knee cartilage. *Magy Seb* 1954;7(5):331–9.
5. Boven F, Bellemans MA, Geurts J, et al. The value of computed tomography scanning in chondromalacia patellae. *Skeletal Radiol* 1982;8(3):183–5.
6. Boven F, Bellemans MA, Geurts J, et al. A comparative study of the patello-femoral joint on axial roentgenogram, axial arthrogram, and computed tomography following arthrography. *Skeletal Radiol* 1982;8(3):179–81.
7. Reiser M, Karpf PM, Bernett P. Diagnosis of chondromalacia patellae using CT arthrography. *Eur J Radiol* 1982;2(3):181–6.
8. Buckwalter KA. CT arthrography. *Clin Sports Med* 2006;25(4):899–915.
9. Lecouvet FE, Simoni P, Koutassisoff S, et al. Multidetector spiral CT arthrography of the shoulder: Clinical applications and limits, with MR arthrography and arthroscopic correlations. *Eur J Radiol* 2008;68(1):120–36.
10. Hall FM, Goldberg RP, Wyshak G, et al. Shoulder arthrography: comparison of morbidity after use of various contrast media. *Radiology* 1985;154(2):339–41.
11. Lecouvet F, Dorzée B, Dubuc J, et al. Cartilage lesions of the glenohumeral joint: diagnostic effectiveness of multidetector spiral CT arthrography and comparison with arthroscopy. *Eur Radiol* 2007;17(7):1763–71.
12. Railhac J. Iopentol (Imagopaque 300) compared with ioxaglate (Hexabrix 320) in knee arthrography. A clinical trial assessing immediate and late adverse events and diagnostic information. *Eur Radiol* 1997;7(4):S135–9.
13. Vande Berg BC, Lecouvet F, Malghem J. Frequency and topography of lesions of the femoro-tibial cartilage at spiral CT arthrography of the knee: a study in patients with normal knee radiographs and without history of trauma. *Skeletal Radiol* 2002;31(11):643–9.
14. Noël C, Campagna R, Minoui A, et al. Fissures of the posterior labrum and associated lesions: CT arthrogram evaluation. *J Radiol* 2008;89(4):487–93.
15. Daenen BR, Ferrara MA, Marcelis S, et al. Evaluation of patellar cartilage surface lesions: comparison of CT arthrography and fat-suppressed FLASH 3D MR imaging. *Eur Radiol* 1998;8(6):981–5.
16. Binkert CA, Verdun FR, Zanetti M, et al. Arthrography of the glenohumeral joint: CT fluoroscopy versus conventional CT and fluoroscopy—comparison of image-guidance techniques. *Radiology* 2003;229(1):153–8.
17. Wyler A, Bousson V, Bergot C, et al. Hyaline cartilage thickness in radiographically normal cadaveric hips: comparison of spiral CT arthrographic and macroscopic measurements. *Radiology* 2007;242(2):441–9.
18. Osinski T, Malfair D, Steinbach L. Magnetic resonance arthrography. *Orthop Clin North Am* 2006;37(3):299–319, vi.
19. Hajek PC, Sartoris DJ, Neumann CH, et al. Potential contrast agents for MR arthrography: in vitro evaluation and practical observations. *Am J Roentgenol* 1987;149(1):97–104.
20. Zanetti M, Hodler J. Contrast media in MR arthrography of the glenohumeral joint: intra-articular gadopentetate vs saline: preliminary results. *Eur Radiol* 1997;7(4):498–502.
21. Binkert CA, Zanetti M, Gerber C, et al. MR arthrography of the glenohumeral joint: two concentrations of gadoteridol versus ringer solution as the intraarticular contrast material. *Radiology* 2001;220(1):219–24.
22. Schulte-Altendorneburg G, Gebhard, et al. MR arthrography: pharmacology, efficacy and safety in clinical trials. *Skeletal Radiol* 2003;32(1):1–12.
23. Hodler J. Technical errors in MR arthrography. *Skeletal Radiol* 2008;37(1):9–18.
24. Masi JN, Newitt D, Sell CA, et al. Optimization of gadodiamide concentration for MR arthrography at 3 T. *Am J Roentgenol* 2005;184(6):1754–61.
25. Andreisek G, Froehlich JM, Hodler J, et al. Direct MR arthrography at 1.5 and 3.0 T: signal dependence on gadolinium and iodine concentrations—phantom study. *Radiology* 2008;247(3):706–16.
26. Detreille R, Sauer B, Zabel JP, et al. [Technical considerations for injection of a mixture of iodinated contrast material and Artirem for combined CT and MR arthrography]. *J Radiol* 2007;88(6):863–9.
27. Brown RR, Clarke DW, Daffner RH. Is a mixture of gadolinium and iodinated contrast material safe during MR arthrography? *Am J Roentgenol* 2000;175(4):1087–90.
28. Choi JY, Kang HS, Hong SH, et al. Optimization of the contrast mixture ratio for simultaneous direct MR and CT arthrography: an in vitro study. *Korean J Radiol* 2008;9(6):520–5.

29. Kopka L, Funke M, Fischer U, et al. MR arthrography of the shoulder with gadopentetate dimeglumine: influence of concentration, iodinated contrast material, and time on signal intensity. *Am J Roentgenol* 1994;163(3):621–3.
30. Jacobson JA, Lin J, Jamadar DA, et al. Aids to successful shoulder arthrography performed with a fluoroscopically guided anterior approach. *Radiographics* 2003;23(2):373–8.
31. Mulligan ME. CT-guided shoulder arthrography at the rotator cuff interval. *Am J Roentgenol* 2008;191(2):W58–61.
32. Koivikko MP, Mustonen AO. Shoulder magnetic resonance arthrography: a prospective randomized study of anterior and posterior ultrasonography-guided contrast injections. *Acta Radiol* 2008;49(8):912–7.
33. Lohman M, Vasenius J, Nieminen O. Ultrasound guidance for puncture and injection in the radiocarpal joint. *Acta Radiol* 2007;48(7):744–7.
34. Rutten M, Collins J, Maresch B, et al. Glenohumeral joint injection: a comparative study of ultrasound and fluoroscopically guided techniques before MR arthrography. *Eur Radiol* 2009;19(3):722–30.
35. Petersilge CA, Lewin JS, Duerk JL, et al. MR arthrography of the shoulder: rethinking traditional imaging procedures to meet the technical requirements of MR imaging guidance. *Am J Roentgenol* 1997;169(5):1453–7.
36. Berná-Serna JD, Redondo MV, Martínez F, et al. A simple technique for shoulder arthrography. *Acta Radiol* 2006;47(7):725–9.
37. Catalano OA, Manfredi R, Vanzulli A, et al. MR arthrography of the glenohumeral joint: modified posterior approach without imaging guidance. *Radiology* 2007;242(2):550–4.
38. DeMouy EH, Menendez CV, Bodin CJ. Palpation-directed (non-fluoroscopically guided) saline-enhanced MR arthrography of the shoulder. *Am J Roentgenol* 1997;169(1):229–31.
39. Freiburger RH. *Arthrography*. Upper Saddle River (NJ): Prentice Hall; 1979.
40. Chevrot A, Pallardy G. *Arthrographies opaques*. Masson; 1988.
41. Crim J. *Arthrography: principles & practice in radiology*. Lippincott Williams & Wilkins; 2008.
42. Obermann WR, Bloem JL, Hermans J. Knee arthrography: comparison of iotrolan and ioxaglate sodium meglumine. *Radiology* 1989;173(1):197–201.
43. Andreisek G, Duc SR, Froehlich JM, et al. MR arthrography of the shoulder, hip, and wrist: evaluation of contrast dynamics and image quality with increasing injection-to-imaging time. *Am J Roentgenol* 2007;188(4):1081–8.
44. Wagner SC, Schweitzer ME, Weishaupt D. Temporal behavior of intraarticular gadolinium. *J Comput Assist Tomogr* 2001;25(5):661–70.
45. Mutschler C, Vande Berg BC, Lecouvet FE, et al. Postoperative meniscus: assessment at dual-detector row spiral CT arthrography of the knee. *Radiology* 2003;228(3):635–41.
46. Spataro RF, Katzberg RW, Burgener FA, et al. Epinephrine enhanced knee arthrography. *Invest Radiol* 1978;13(4):286–90.
47. Hall FM. Epinephrine-enhanced knee arthrography. *Radiology* 1974;111(1):215–7.
48. Chung CB, Isaza IL, Angulo M, et al. MR arthrography of the knee: how, why, when. *Radiol Clin North Am* 2005;43(4):733–46, viii–ix.
49. Brenner ML, Morrison WB, Carrino JA, et al. Direct MR arthrography of the shoulder: is exercise prior to imaging beneficial or detrimental? *Radiology* 2000;215(2):491–6.
50. Vande Berg BC, Lecouvet FE, Poilvache P, et al. Spiral CT arthrography of the knee: technique and value in the assessment of internal derangement of the knee. *Eur Radiol* 2002;12(7):1800–10.
51. Rydberg J, Buckwalter KA, Caldemeyer KS, et al. Multisection CT: scanning techniques and clinical applications. *Radiographics* 2000;20(6):1787–806.
52. Baert A, Tack D, Gevenois P. Radiation dose from adult and pediatric multidetector computed tomography. Springer; 2007.
53. Lee M, Kim S, Lee S, et al. Overcoming artifacts from metallic orthopedic implants at high-field-strength MR imaging and multi-detector CT. *Radiographics* 2007;27(3):791–803.
54. Vande Berg B, Malghem J, Maldague B, et al. Multi-detector CT imaging in the postoperative orthopedic patient with metal hardware. *Eur J Radiol* 2006;60(3):470–9.
55. Elentuck D, Palmer WE. Direct magnetic resonance arthrography. *Eur Radiol* 2004;14(11):1956–67.
56. Wutke R, Fellner FA, Fellner C, et al. Direct MR arthrography of the shoulder: 2D vs. 3D gradient-echo imaging. *Magn Reson Imaging* 2001;19(9):1183–91.
57. Newberg AH, Munn CS, Robbins AH. Complications of arthrography. *Radiology* 1985;155(3):605–6.
58. Berquist TH. Imaging of articular pathology: MRI, CT, arthrography. *Clin Anat* 1997;10(1):1–13.
59. Cerezal L, Abascal F, García-Valtuille R, et al. Ankle MR arthrography: how, why, when. *Radiol Clin North Am* 2005;43(4):693–707, viii.
60. Saupé N, Zanetti M, Pfirrmann CWA, et al. Pain and other side effects after MR arthrography: prospective evaluation in 1085 patients. *Radiology* 2009;250(3):830–8.
61. Binkert CA, Zanetti M, Hodler J. Patient's assessment of discomfort during MR arthrography of the shoulder. *Radiology* 2001;221(3):775–8.
62. Blum AG, Simon JM, Cotten A, et al. Comparison of double-contrast CT arthrography image quality with nonionic contrast agents: isotonic dimeric iodixanol

- 270 mg I/mL and monomeric iohexol 300 mg I/mL. *Invest Radiol* 2000;35(5):304–10.
63. Corbetti F, Malatesta V, Camposampiero A, et al. Knee arthrography: effects of various contrast media and epinephrine on synovial fluid. *Radiology* 1986;161(1):195–8.
 64. El-Khoury GY, Alliman KJ, Lundberg HJ, et al. Cartilage thickness in cadaveric ankles: measurement with double-contrast multi-detector row CT arthrography versus MR imaging. *Radiology* 2004;233(3):768–73.
 65. Haubner M, Eckstein F, Schnier M, et al. A non-invasive technique for 3-dimensional assessment of articular cartilage thickness based on MRI part 2: validation using CT arthrography. *Magn Reson Imaging* 1997;15(7):805–13.
 66. Anderson AE, Ellis BJ, Peters CL, et al. Cartilage thickness: factors influencing multidetector CT measurements in a phantom study. *Radiology* 2008;246(1):133–41.
 67. Wyler A, Bousson V, Bergot C, et al. Comparison of MR-arthrography and CT-arthrography in hyaline cartilage-thickness measurement in radiographically normal cadaver hips with anatomy as gold standard. *Osteoarthritis Cartilage* 2009;17(1):19–25.
 68. Schmid MR, Pfirrmann CWA, Hodler J, et al. Cartilage lesions in the ankle joint: comparison of MR arthrography and CT arthrography. *Skeletal Radiol* 2003;32(5):259–65.
 69. Ihara H. Double-contrast CT arthrography of the cartilage of the patellofemoral joint. *Clin Orthop Relat Res* 1985;198:50–5.
 70. Noyes FR, Stabler CL. A system for grading articular cartilage lesions at arthroscopy. *Am J Sports Med* 1989;17(4):505–13.
 71. Outerbridge RE. The etiology of chondromalacia patellae. *J Bone Joint Surg Br* 1961;43-B:752–7.
 72. Vande Berg BC, Lecouvet FE, Poilvache P, et al. Assessment of knee cartilage in cadavers with dual-detector spiral CT arthrography and MR imaging. *Radiology* 2002;222(2):430–6.
 73. Schmid MR, Notzli HP, Zanetti M, et al. Cartilage lesions in the hip: diagnostic effectiveness of MR arthrography. *Radiology* 2003;226(2):382–6.
 74. Llopis E, Cerezal L, Kassarian A, et al. Direct MR arthrography of the hip with leg traction: feasibility for assessing articular cartilage. *Am J Roentgenol* 2008;190(4):1124–8.
 75. McCauley TR, Kornaat PR, Jee W. Central osteophytes in the knee: prevalence and association with cartilage defects on MR imaging. *Am J Roentgenol* 2001;176(2):359–64.
 76. Guermazi A, Burstein D, Conaghan P, et al. Imaging in osteoarthritis. *Rheum Dis Clin North Am* 2008;34(3):645–87.
 77. Brandt KD, Radin EL, Dieppe PA, et al. Yet more evidence that osteoarthritis is not a cartilage disease. *Ann Rheum Dis* 2006;65(10):1261–4.
 78. Yu WK, Bartlett JM, van Sickle DC, et al. Biodistribution of bis-[beta-(N, N, N-trimethylamino)ethyl]-selenide-75Se diiodide, a potential articular cartilage imaging agent. *Int J Rad Appl Instrum B* 1988;15(2):229–30.
 79. Yu SW, Shaw SM, Van Sickle DC. Radionuclide studies of articular cartilage in the early diagnosis of arthritis in the rabbit. *Ann Acad Med Singapore* 1999;28(1):44–8.
 80. Yu WK, Shaw SM, Bartlett JM, et al. The biodistribution of [75Se]bis-[beta-(N, N, N-trimethylamino)ethyl]selenide diiodide in adult guinea pigs. *Int J Rad Appl Instrum B* 1989;16(3):255–9.
 81. Etchebehere EC, Etchebehere M, Gamba R, et al. Orthopedic pathology of the lower extremities: scintigraphic evaluation in the thigh, knee, and leg. *Semin Nucl Med* 1998;28(1):41–61.
 82. Merrick MV. Investigation of joint disease. *Eur J Nucl Med Mol Imaging* 1992;19(10):894–901.
 83. Klingensmith W III, Eshima D, Goddard J. Nuclear medicine procedure manual. 2006th edition. Englewood (CO): Wick Publishing; 2006.
 84. Grant FD, Fahey FH, Packard AB, et al. Skeletal PET with 18F-fluoride: applying new technology to an old tracer. *J Nucl Med* 2008;49(1):68–78.
 85. Beebe M, Dalton J, Espronceda M. CPT 2009 professional edition. American Medical Association; 2009.
 86. Rosenthal L. Nuclear medicine techniques in arthritis. *Rheum Dis Clin North Am* 1991;17(3):585–97.
 87. Love C, Tomas MB, Tronco GG, et al. FDG PET of infection and inflammation. *Radiographics* 2005;25(5):1357–68.
 88. Filippi L, Schillaci O. Usefulness of hybrid SPECT/CT in 99mTc-HMPAO-labeled leukocyte scintigraphy for bone and joint infections. *J Nucl Med* 2006;47(12):1908–13.
 89. Elgazzar AH. The pathophysiologic basis of nuclear medicine. 2nd edition. Berlin, Germany: Springer-Verlag; 2006.
 90. Frauwirth KA, Thompson CB. Regulation of T lymphocyte metabolism. *J Immunol* 2004;172(8):4661–5.
 91. Kostakoglu L, Agress H, Goldsmith SJ. Clinical role of FDG PET in evaluation of cancer patients. *Radiographics* 2003;23(2):315–40.
 92. Nakamura H, Masuko K, Yudoh K, et al. Positron emission tomography with 18F-FDG in osteoarthritic knee. *Osteoarthritis Cartilage* 2007;15(6):673–81.
 93. Wandler E, Kramer EL, Sherman O, et al. Diffuse FDG shoulder uptake on PET is associated with

- clinical findings of osteoarthritis. *Am J Roentgenol* 2005;185(3):797–803.
94. Elzinga E, van der Laken C, Comans E, et al. 2-Deoxy-2-[F-18]fluoro-D-glucose joint uptake on positron emission tomography images: rheumatoid arthritis versus osteoarthritis. *Mol Imaging Biol* 2007;9(6):357–60.
 95. Sarikaya I, Sarikaya A, Holder LE. The role of single photon emission computed tomography in bone imaging. *Semin Nucl Med* 2001;31(1):3–16.
 96. Bahk Y, Kim S, Chung S, et al. Dual-head pinhole bone scintigraphy. *J Nucl Med* 1998;39(8):1444–8.
 97. Townsend DW, Carney JP, Yap JT, et al. PET/CT today and tomorrow. *J Nucl Med* 2004;45(1 suppl):4S–14S.
 98. Horger M, Eschmann SM, Pfannenbergs C, et al. Evaluation of combined transmission and emission tomography for classification of skeletal lesions. *Am J Roentgenol* 2004;183(3):655–61.
 99. Strobel K, Burger C, Seifert B, et al. Characterization of focal bone lesions in the axial skeleton: performance of planar bone scintigraphy compared with SPECT and SPECT fused with CT. *Am J Roentgenol* 2007;188(5):W467–74.
 100. Buck AK, Nekolla S, Ziegler S, et al. SPECT/CT. *J Nucl Med* 2008;49(8):1305–19.
 101. Even-Sapir E, Flusser G, Lerman H, et al. SPECT/multislice low-dose CT: a clinically relevant constituent in the imaging algorithm of nononcologic patients referred for bone scintigraphy. *J Nucl Med* 2007;48(2):319–24.
 102. Taft L. Positron emission tomography (PET) and mammography (PEM) for breast cancer: importance to surgeons. *Ann Surg Oncol* 2007;14(1):3–13.
 103. Naviscan - home. Available at: <http://www.naviscan.com>. Accessed January 27, 2009.
 104. Duncan I, Dorai-Raj A, Khoo K, et al. The utility of bone scans in rheumatology. *Clin Nucl Med* 1999;24(1):9–14.
 105. Duer A, Ostergaard M, Horslev-Petersen K, et al. Magnetic resonance imaging and bone scintigraphy in the differential diagnosis of unclassified arthritis. *Ann Rheum Dis* 2008;67(1):48–51.
 106. Hutton CW, Higgs ER, Jackson PC, et al. 99mTc HMDP bone scanning in generalised nodal osteoarthritis. II. The four hour bone scan image predicts radiographic change. *Ann Rheum Dis* 1986;45(8):622–6.
 107. Buckland-Wright C. Current status of imaging procedures in the diagnosis, prognosis and monitoring of osteoarthritis. *Baillieres Clin Rheumatol* 1997;11(4):727–48.
 108. Mazzuca SA, Brandt KD, Schauwecker DS, et al. Bone scintigraphy is not a better predictor of progression of knee osteoarthritis than Kellgren and Lawrence grade. *J Rheumatol* 2004;31(2):329–32.
 109. Boegård T. Radiography and bone scintigraphy in osteoarthritis of the knee—comparison with MR imaging. *Acta Radiol Suppl* 1998;418:7–37.
 110. Dieppe P, Cushnaghan J, Young P, et al. Prediction of the progression of joint space narrowing in osteoarthritis of the knee by bone scintigraphy. *Ann Rheum Dis* 1993;52(8):557–63.
 111. Mazzuca SA, Brandt KD, Schauwecker DS, et al. Severity of joint pain and Kellgren-Lawrence grade at baseline are better predictors of joint space narrowing than bone scintigraphy in obese women with knee osteoarthritis. *J Rheumatol* 2005;32(8):1540–6.
 112. De Maeseneer M, Lenchik L, Everaert H, et al. Evaluation of lower back pain with bone scintigraphy and SPECT. *Radiographics* 1999;19(4):901–12.
 113. Dolan AL, Ryan PJ, Arden NK, et al. The value of SPECT scans in identifying back pain likely to benefit from facet joint injection. *Rheumatology* 1996;35(12):1269–73.
 114. Kim CK, Park KW. Characteristic appearance of facet osteoarthritis of the lower lumbar spine on planar bone scintigraphy with a high negative predictive value for metastasis. *Clin Nucl Med* 2008;33(4):251–4.
 115. Kim H, So Y, Moon S, et al. Clinical value of 99mTc-methylene diphosphonate (MDP) bone single photon emission computed tomography (SPECT) in patients with knee osteoarthritis. *Osteoarthritis Cartilage* 2008;16(2):212–8.
 116. Jeer PJ, Mahr CC, Keene GC, et al. Single photon emission computed tomography in planning unicompartmental knee arthroplasty. A prospective study examining the association between scan findings and intraoperative assessment of osteoarthritis. *Knee* 2006;13(1):19–25.
 117. Van der Wall H, Fogelman I. Scintigraphy of benign bone disease. *Semin Musculoskelet Radiol* 2007;11(4):281–300.
 118. Vanhove C, Andreyev A, Defrise M, et al. Resolution recovery in pinhole SPECT based on multi-ray projections: a phantom study. *Eur J Nucl Med Mol Imaging* 2007;34(2):170–80.
 119. Beekman FJ, Kamphuis C, King MA, et al. Improvement of image resolution and quantitative accuracy in clinical single photon emission computed tomography. *Comput Med Imaging Graph* 2001;25(2):135–46.